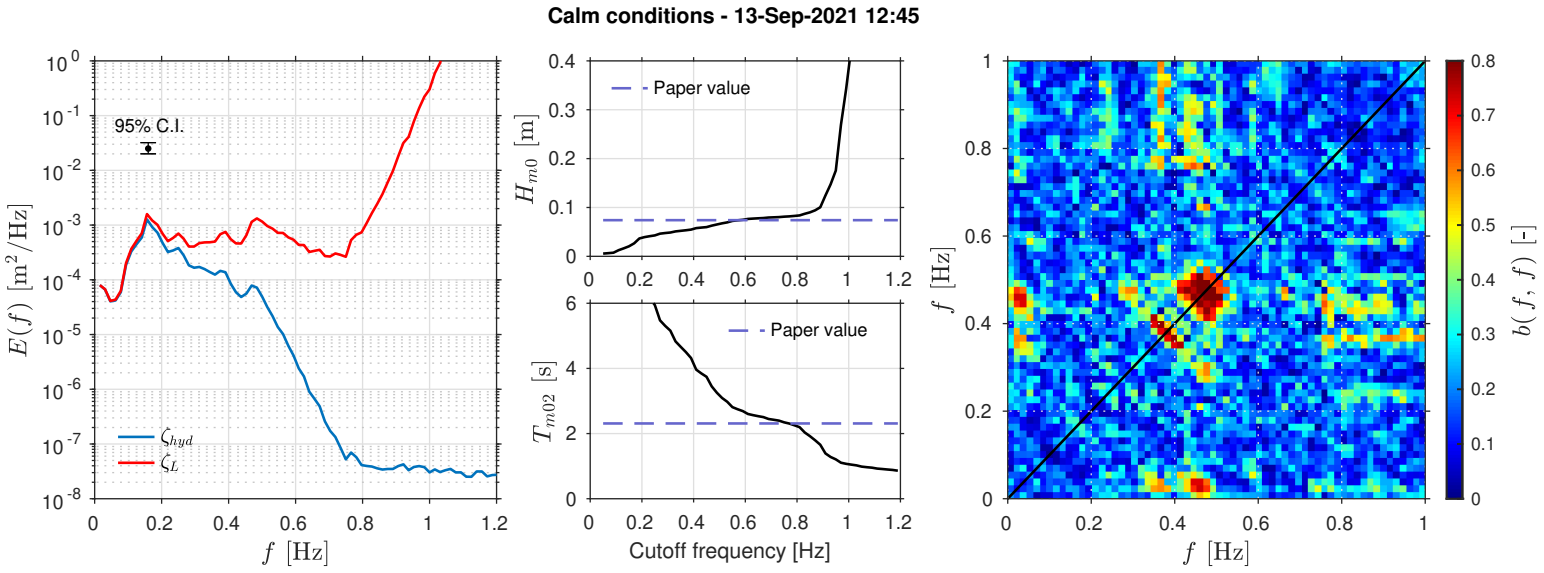

Figure 1: Reconstruction analysis for the calm conditions of 13 September 2021 at 12:45. The left panel shows the surface elevation energy density spectra *E* for the two reconstructions (hydrostatic and linear). The central panels shows the sensitivity of the bulk parameters H_{m0} and T_{m02} to the choice of the high cutoff frequency in the integral for computing moments. The right panel shows the bicoherence of the hydrostatic reconstruction.

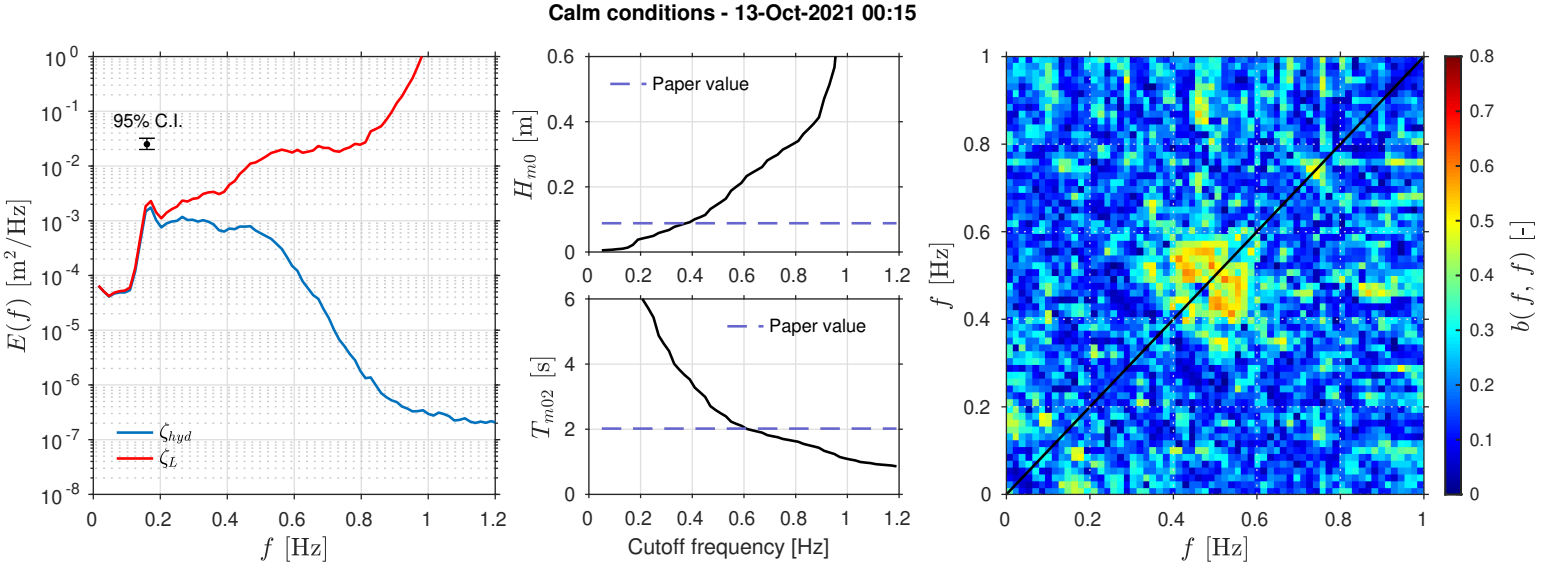

Figure 2: Reconstruction analysis for the calm conditions of 13 October 2021 at 00:15. The left panel shows the surface elevation energy density spectra *E* for the two reconstructions (hydrostatic and linear). The central panels shows the sensitivity of the bulk parameters H_{m0} and T_{m02} to the choice of the high cutoff frequency in the integral for computing moments. The right panel shows the bicoherence of the hydrostatic reconstruction.

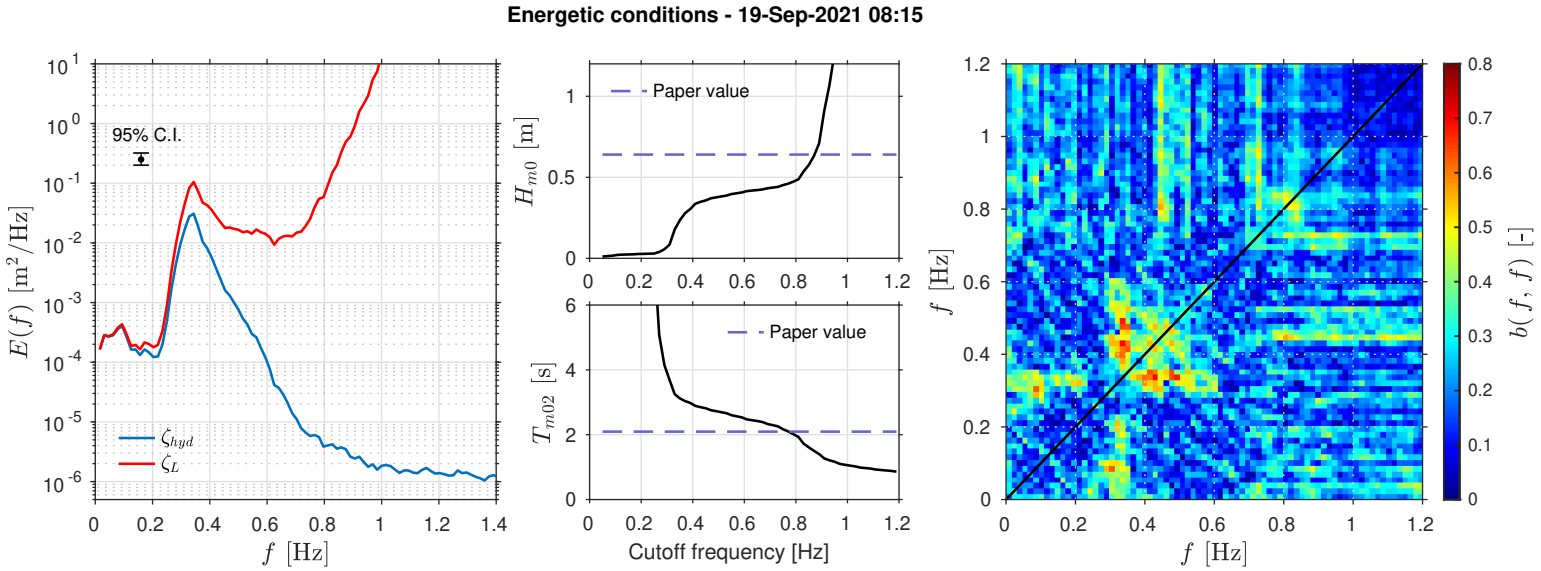

Figure 3: Reconstruction analysis for the energetic conditions of 19 September 2021 at 08:15 (conditions of Figure 8 in the paper). The left panel shows the surface elevation energy density spectra *E* for the two reconstructions (hydrostatic and linear). The central panels shows the sensitivity of the bulk parameters H_{m0} and T_{m02} to the choice of the high cutoff frequency in the integral for computing moments. The right panel shows the bicoherence of the hydrostatic reconstruction.

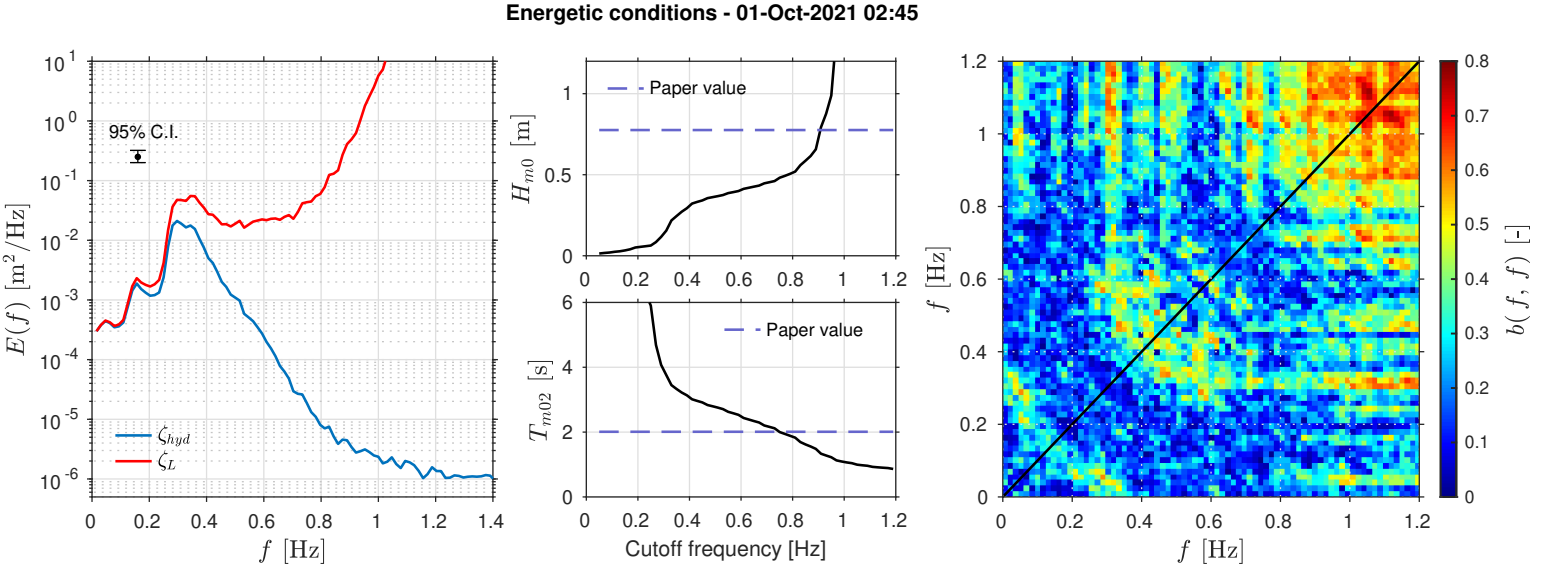

Figure 4: Reconstruction analysis for the energetic conditions of 1 October 2021 at 02:45. The left panel shows the surface elevation energy density spectra *E* for the two reconstructions (hydrostatic and linear). The central panels shows the sensitivity of the bulk parameters H_{m0} and T_{m02} to the choice of the high cutoff frequency in the integral for computing moments. The right panel shows the bicoherence of the hydrostatic reconstruction.